Competition between a Macroion and a Polyelectrolyte in Complexation with an Oppositely Charged Polyelectrolyte

Marie Skepö*

Health and Society, Malmö University, S-205 06 Malmö, Sweden

Received: September 18, 2003; In Final Form: January 15, 2004

The competition between a spherical macroion and a polyelectrolyte in complexation with an oppositely charged flexible polyelectrolyte has been studied by means of Monte Carlo simulations. A simple model system with focus on the electrostatic interactions has been used to investigate under what conditions the macroion in a polyelectrolyte−macroion complex (excess of polyelectrolyte charges) is exchanged with a polyelectrolyte. It is shown that the macroion is released when the charge of the added polyelectrolyte equals or exceeds that of the polyelectrolyte in the complex. The effect of the polyelectrolyte length, flexibility, and linear charge density on the macroion release has been investigated.

1. Introduction

The understanding of the complexation between polyelectrolytes and oppositely charged macroions is of great importance in many biological and technological applications, mainly because polyelectrolytes (PEs) display a high solubility in water and strong adsorbing capacity on surfaces bearing an opposite charge. An interesting feature is that they can act both as stabilizing and as destabilizing agents in particle suspensions. In aqueous solutions, polyelectrolytes may interact strongly with other macroions and, in particular, they tend to associate with objects of opposite charge and form complexes. Examples include synthetic polyelectrolytes adsorbing on colloidal particles,[1] surfactant micelles,[2] and proteins,[3,4] as well as the complexation of DNA with latex particles,[5] dendrimers,[6] and proteins.[7,8] Applications of complexes made by synthetic polyelectrolytes and macroions include the control of dispersion stabilization, flocculation, and precipitation, while complexes consisting of biological polyelectrolytes and macroions are used, for example, for the immobilization of enzymes and purification of proteins.

The complexation between a polyelectrolyte and a macroion has been intensively studied during the last years. Some of the experimental studies have been reviewed,[2,9−11] and a lot of work also concerns computer simulations[12−20] and theory.[21−28] Several simulation studies have also addressed the complexation between one polyelectrolyte and several macroions,[24,29−33] and recently solutions containing polyelectrolytes and macroions.[34] The complexation of two/several oppositely charged polyelectrolytes has also been studied,[35] but so far the competition between two like charged species, that is, a polyelectrolyte and a macroion, in complexation with an oppositely charged polyelectrolyte has not been investigated.

This paper will focus on what happens to a 1:1 polyelectrolyte (PE_{host})−macroion (M) complex, where $Z_M < Z_{host}$ (the macroion charge is less than the PE_{host} charge), upon addition of a guest polyelectrolyte (PE_{guest}) of the same sign of charge as the macroion. This is an important question where exchange reactions are applied, for example, in protein purification, drug delivery, or wastewater treatment. Obviously, there are three options: (i) $PE_{host}-M + PE_{guest} \rightarrow PE_{host}-M + PE_{guest}$ (nothing changes), (ii) $PE_{host}-M + PE_{guest} \rightarrow PE_{host}-PE_{guest} + M$ (the macroion is exchanged by the guest polyelectrolyte), or (iii) $PE_{host}-M + PE_{guest} \rightarrow PE_{host}-PE_{guest}-M$ (one large complex is created).

The main questions studied for the system upon addition of the PE_{guest} concern the complex composition and structure and the circumstances under which the macroion is released. This has been investigated by performing systematic changes in the chain properties of the PE_{guest}, in particular, length, linear charge density, and flexibility. The equilibrium properties of the model systems were obtained by using canonical Monte Carlo simulations according to the Metropolis algorithm.

The outline of the paper is as follows: The model and some simulation aspects are given in section 2. In section 3, the results are presented and discussed, and the article ends with conclusions given in section 4.

2. Method

2.1. Model. The influence of an added PE_{guest} to a solution containing one PE_{host} and one oppositely charged macroion has been investigated using the primitive model. In the primitive model, all particles are represented as hard charged spheres with different charges and sizes, and the solvent, in this case water, is replaced by its relative permittivity.

The model contains four different types of particles: (i) connected spheres representing hydrophilic linear polyelectrolytes, (ii) a larger unconnected sphere representing a macroion, (iii) small unconnected spheres representing small positive ions (cations), and (iv) small unconnected spheres representing small negative ions (anions). The polyelectrolytes are described as freely jointed chains of charged hard spheres (segments) connected by harmonic bonds with their intrinsic chain flexibilities regulated by harmonic angular energy terms.

The total potential energy of the system is given by

$$U = U_{\text{nonbond}} + U_{\text{bond}} + U_{\text{angle}} \quad (1)$$

where the nonbonded energy is assumed to be pairwise additive according to

* Corresponding author. E-mail: marie.skepo@ts.mah.se.

10.1021/jp036789s CCC: $27.50
Published on Web 04/06/2004

$$U_{\text{nonbond}} = \sum_{i<j} u_{ij} \tag{2}$$

Within the primitive model, the interaction potential, u_{ij}, for pair ij, where i and j denote a polyelectrolyte segment (seg), a macroion (M), a cation, or an anion, is given by

$$u_{ij}(r_{ij}) = \begin{cases} \infty & r_{ij} < R_i + R_j \\ \dfrac{Z_i Z_j e^2}{4\pi\epsilon_0\epsilon_r} \dfrac{1}{r_{ij}} & r_{ij} \geq R_i + R_j \end{cases} \tag{3}$$

where Z_i is the charge of particle i, R_i is the radius of particle i, e is the elementary charge, ϵ_0 is the permittivity of vacuum, ϵ_r is the permittivity of water, and $r_{ij} \equiv |\mathbf{r}_j - \mathbf{r}_i|$, the distance between the centers of particles i and j, with $\mathbf{r}_i$ denoting the position of particle i. The relative permittivity is constant throughout the system, and hence, surface polarization is neglected.

The remaining two terms in eq 1 are the bond and angular energy potentials, which apply only to the polyelectrolytes. The bond energy is given by

$$U_{\text{bond}} = \sum_{i=1}^{N_{\text{seg}}-1} \frac{k_{\text{bond}}}{2}(r_{i,i+1} - r_0)^2 \tag{4}$$

where $r_{i,i+1}$ denotes the distance between two connected segments with the reference separation $r_0 = 5$ Å and the force constant $k_{\text{bond}} = 0.4$ N/m and where N_{seg} denotes the number of segments of the polyelectrolyte. The angular energy is represented by

$$U_{\text{angle}} = \sum_{i=2}^{N_{\text{seg}}-1} \frac{k_{\text{ang}}}{2}(\alpha_i - \alpha_0)^2 \tag{5}$$

where α_i is the angle formed by vectors $(\mathbf{r}_{i+1} - \mathbf{r}_i)$ and $(\mathbf{r}_{i-1} - \mathbf{r}_i)$ made by three consecutive segments with the reference angle $\alpha_0 = 180°$ and the force constant k_{ang}. In addition to the angular potential, the electrostatic interaction among the segments also contributes to the rigidity of the polyelectrolyte, and this electrostatic contribution is of course affected by other ionic particles.

The effect of adding a PE_{guest} to a PE_{host}−M complex has been studied. The macroion and PE_{guest} have the same sign of charge, which is opposite to that of the PE_{host}. The reference system consists of one PE_{host} with the chain length $N_{seg,host} = 40$ segments, where each segment has one elementary charge per segment, giving a linear charge density (τ_{host}) of 0.2 e/Å. An oppositely charged macroion is then added with the radius $R_M = 15$ Å and the charge $Z_M = -10$. Hence, $Z_M < Z_{PE}$. This system has been thoroughly studied in earlier papers by Jonsson and Linse.[29,30] To the reference system, eight different PE_{guest}'s have been added with $\tau_{guest} = -0.2$ e/Å and the length $N_{seg,guest} = 0$, 5, 10, 20, 30, 40, 60, and 80 segments, which gives a charge ratio between the polyelectrolytes ($\beta = N_{seg,guest}Z_{guest}/N_{seg,host}Z_{host}$) of $\beta = 0$, 0.125, 0.25, 0.5, 0.75, 1.0, 1.5, and 2.0, respectively. If $\beta < 1$, there is an excess of PE_{host} charges, if $\beta = 1$, there is an equal amount of PE_{host} and PE_{guest} charges (stoichiometric charge neutral), and for $\beta > 1$, there is an excess of PE_{guest} charges. All counterions are treated explicitly. If nothing else is stated, an angular force constant of $k_{ang} = 0$ is used for both of the polyelectrolytes, which gives totally flexible chains and a bare persistence length[40] of $l_p = 7$ Å. The charged species are enclosed in a cubic box with the box length $L = 300$ Å, corresponding to the macroion volume fraction $\phi_M = (4\pi/3)R_M^3\rho_M = 5.2 \times 10^{-4}$, with $\rho_M = N_M/L^3$. Throughout, $T = 298$ K and $\epsilon_r = 78.4$, thus representing water at ambient temperature. Parameters of the studied systems are given in Table 1.

TABLE 1: General Data of the Model

box length	$L = 300$ Å
macroion radius	$R_M = 15$ Å
segment radius	$R_{seg} = 2$ Å
small ion radius	$R_{ion} = 2$ Å
macroion charge	$Z_M = -10$
segment charge	$Z_{seg} = -2, -1, -0.5, -0.25, 1$
small ion charge	$Z_{ion} = \pm 1$
no. of segments	$N_{seg} = 5$, 10, 20, 30, 40, 60, 80
no. of macroions	$N_M = 1$
no. of cations	$N_{cation} = 0-90$
no. of anions	$N_{anion} = 40$
temperature	$T = 298$ K
permittivity of water	$\epsilon_r = 78.4$

2.2. Simulation Aspects. The equilibrium properties of the model systems were obtained from canonical Monte Carlo (MC) simulations according to the Metropolis algorithm.[36,37] The particles were enclosed in a cubic box, and periodical boundary conditions were applied. The long-ranged Coulomb interactions were handled by using the Ewald summation technique with conduction boundary conditions (see refs 29 and 30 for further details). The examination of the configurational space was accelerated by using four different types of displacements of the polyelectrolyte: (i) translational displacement of the single charged particle, (ii) pivot rotation of a part of the polyelectrolyte chain, (iii) translation of the entire polyelectrolyte chain, and (iv) slithering movement using a biased sampling technique. The probabilities of different trial moves were selected to enable single particle moves 20 times more often than pivot movements and translation of the entire chain and 10 times more often than slithering movements. The particles were initially placed randomly in the simulation box, and after equilibrium, the length of a production run was at least 2×10^6 MC trial moves per particle. Despite the strong polyelectrolyte−macroion complex, it has previously been shown that the present protocol produces an ergodic sampling for one polyelectrolyte and several macroions[29,30] and for oppositely charged polyelectrolytes.[38]

The reported uncertainty of simulated quantities is one standard deviation of the mean as estimated by dividing the simulations into 10 subbatches. Selected uncertainty bars are given. The simulations were performed by applying the integrated Monte Carlo/molecular dynamics/Brownian dynamics simulation package Molsim.[39]

3. Results and Discussion

3.1. Reference System. The effect of adding one PE_{guest} to a system consisting of a PE_{host}−M complex will first be presented from typical configurations of the system; see Figure 1. The complexation between the PE_{host} and the macroion has been studied in detail in earlier papers.[29,30] When a small PE_{guest} of 10 segments is added to the system (Figure 1a), the PE_{host} seems to complex with both of them and the macroion is located in the end of the chain. An increase in $N_{seg,guest}$ of the PE_{guest} to 30 segments gives rise to one large PE_{host}−PE_{guest}−M complex (Figure 1b), which is charge neutral. When the PE_{host} and the PE_{guest} have the same length and charge (of opposite signs) (Figure 1c), the macroion is completely released from the PE_{host} and both polyelectrolytes have created a charge neutral compact complex. Further addition of segments to the PE_{guest} continues the trend of a totally released macroion and a polyelectrolyte complex (snapshots not shown here).

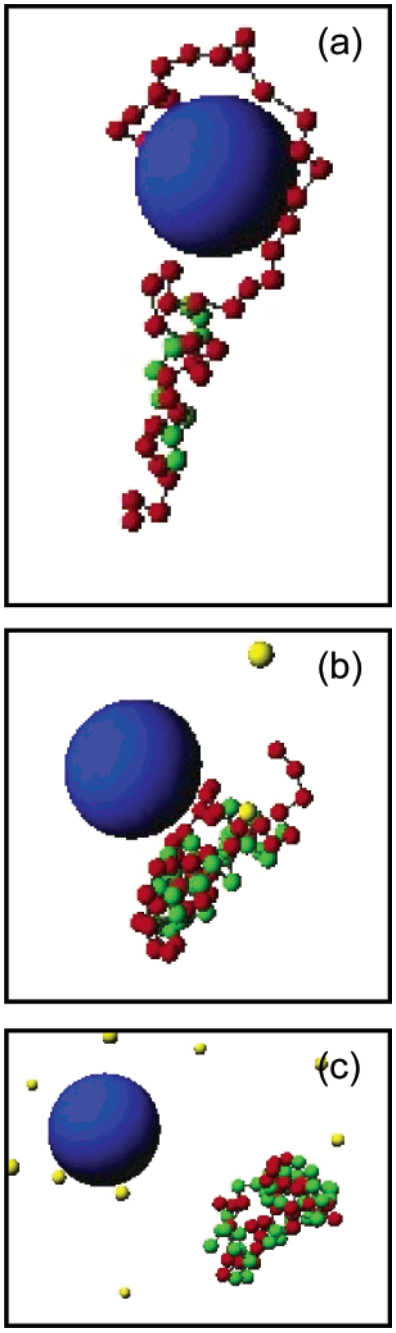

Figure 1. Some typical configurations of the reference system. The simulated systems contain one PE_{host} with 40 segments and the linear charge density 0.2 e/Å (connected red dots) and one oppositely charged macroion (larger blue sphere) with the charge $Z_M = -10$, and (a) $N_{seg,guest} = 10$, (b) $N_{seg,guest} = 30$, and (c) $N_{seg,guest} = 40$ segments in the added PE_{guest} with the linear charge density −0.2 e/Å. Some of the small ions are presented as unconnected yellow dots. Note: the parts of the figure are justified for best visibility. The particle sizes in parts a−c are identical.

3.1.1. Complex Composition. The trends discussed above are more clearly shown in Figure 2, where the number of complexed macroions with the PE_{host} is shown as a function of $N_{seg,guest}$. A geometrical definition has been used to define a complex between the PE_{host} and the macroion, and they are considered complexed if the distance between at least one polyelectrolyte segment and the macroion does not exceed 5 Å from their contact separation. Since there is only one macroion in the system, there will be at most one complex. The function in Figure 2 indicates that the macroion remains complexed with

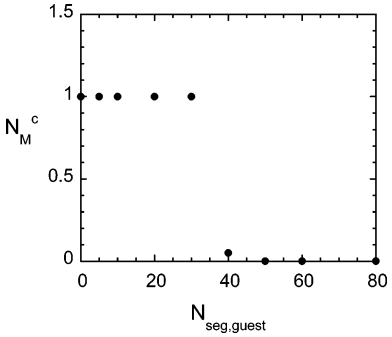

Figure 2. Number of complexed macroions, N_M^c, with the PE_{host} vs $N_{seg,guest}$ for the reference system. The estimated uncertainties are smaller than the sizes of the symbols.

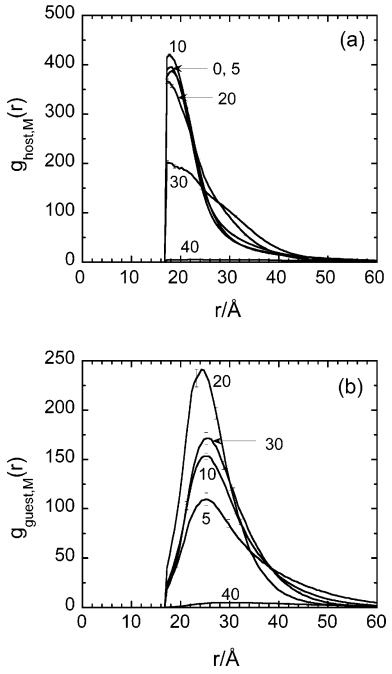

Figure 3. (a) $PE_{host}-M$ $g_{host,M}(r)$ and (b) $PE_{guest}-M$ $g_{guest,M}(r)$ rdf's, at the indicated $N_{seg,guest}$ for the reference system.

the PE_{host} until $N_{seg,guest} = 40$, and then it is released. Hence, the macroion is released when $N_{seg,guest} = N_{seg,host}$ (compare to $N_{seg,host} = 40$).

3.1.2. Structure of the Complex. The complex has been further characterized by the radial distribution functions (rdf's), $g_{ij}(r)$, between $PE_{host}-M$ and $PE_{guest}-M$. The rdf's measure the spatial correlations in real space. $g_{ij}(r)$ expresses the relative density of a particle of type j at a distance r from a given particle of type i; that is, at a short distance, $g_{ij}(r)$ is zero because of hard sphere overlaps, whereas, in a homogeneous solution, it conventionally approaches one at large distances.

Figure 3 shows $g_{host,M}$ and $g_{guest,M}$ for indicated $N_{seg,guest}$. In Figure 3a, and starting with the reference system (no added PE_{guest}), $g_{host,M}$ displays a maximum at 18.25 Å, corresponding to a segment−macroion distance of 1.25 Å. The high amplitude and the width of the maximum indicate that the polyelectrolyte segments are accumulated close to the macroion surface. A short PE_{guest} does not directly influence the behavior (compare to $N_{seg,guest} = 0-20$). When $N_{seg,guest} > 20$, the magnitude of the maximum decreases and the width becomes broader; thus, the $PE_{host}-M$ complex starts to loosen up. When $N_{seg,guest} = 40$, $g_{host,M} \rightarrow 1$, indicating that the macroion is totally released from the PE_{host}. For $N_{seg,guest} > 40$, the PE_{host} is never in contact with

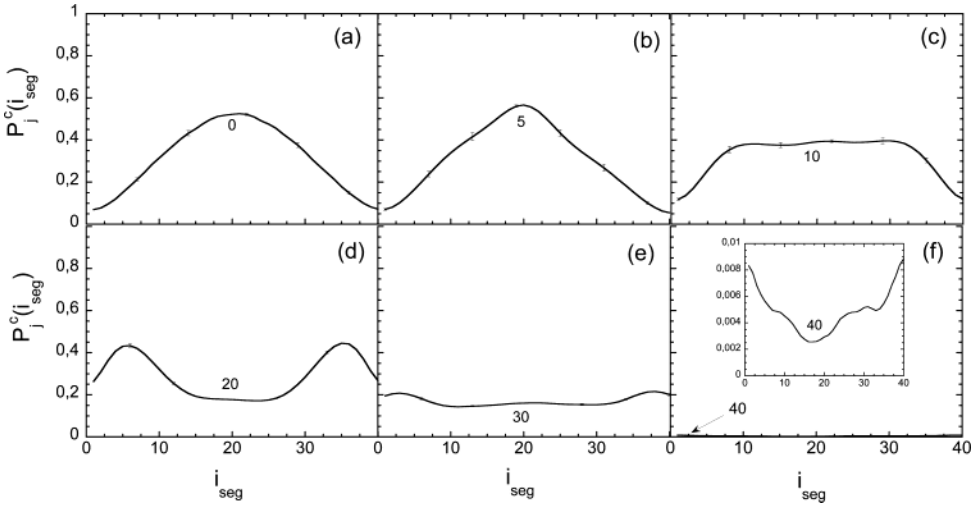

Figure 4. Complexation probability, $P_j^c(i_{seg})$, vs segment rank (i_{seg}) for the reference system with (a) $N_{seg,guest} = 0$, (b) $N_{seg,guest} = 5$, (c) $N_{seg,guest} = 10$, (d) $N_{seg,guest} = 20$, (e) $N_{seg,guest} = 30$, and (f) $N_{seg,guest} = 40$. The inset in part f shows an enlargement.

the macroion. The snapshots in Figure 1 above showed that, up to $N_{seg,guest} = 30$, both the PE_{guest} and the macroion were complexed with the PE_{host}. Figure 3b shows that as long as both the macroion and PE_{guest} are complexed to the PE_{host}, they are complexed at some distance from each other, which indicates repulsive interaction between the species. The maximum occurs at $g_{guest,M} \approx 25$ Å, which gives an average distance of 8 Å between a guest segment and a macroion.

A more detailed analysis of the $PE_{host}-M$ complexation has been performed by analyzing how the macroion is complexed with the PE_{host} and to what degree each segment of the PE_{host} is involved. The probability that segment i_{seg}, where i_{seg} is the segment rank of the PE_{host}, is complexed with macroion j, $P_j^c(i_{seg})$, has been evaluated. The same criterion for the complex as above has been used. The lower limit, $P_j^c(i_{seg}) = 0$, implies that segment i_{seg} is never complexed with macroion j, whereas $P_j^c(i_{seg}) = 1$ means that the segment is always complexed with macroion j. Figure 4 displays the complexation probability, $P_j^c(i_{seg})$, between the PE_{host} and the macroion as a function of i_{seg}, for all added PE_{guest}'s. In the reference system, the complexation probability is completely symmetric with respect to a reflection at $i_{seg} = (N_{seg,host} + 1)/2$ (Figure 4a). This demonstrates that the mobility in the configurational space is sufficient for an adequate sampling of the complexation between the macroion and the different segments of the PE_{host} despite the strong electrostatic macroion−polyelectrolyte interaction ($\approx -40kT$ in total). When $N_{seg,guest}$ is increased, the binding region gets broader, although it is still symmetric. From this analysis, it is shown that the MC simulation protocol used is adequate for obtaining complete equilibrium results with respect to the $PE_{host}-$macroion complexation when PE_{guest}'s are added.

The location of the macroion along the PE_{host} has also been evaluated. Notice that the functions display mirror symmetry with respect to a reflection at $i_{seg} = (N_{seg,host} + 1)/2$, and hence, the two equal halves of the chains experience on average the same environment. Without an added PE_{guest} (Figure 4a), the trend observed is that the macroion prefers to complex with the central segments of the PE_{host} with two dangling tails.[29] When a short PE_{guest} of five segments is added (Figure 4b), the binding region becomes narrower and the amplitude is slightly increased; hence, the PE_{host} creates a more compact surface layer and the $PE_{host}-M$ complex is firmer. For $N_{seg,guest} = 10$, the binding region gets broader and the tails become more involved in the complexation process. When a PE_{guest} of 20 segments is added, two maxima are represented, one in each end of the chain. This indicates that the macroion is preferentially located in one end of the chain, while, for a PE_{guest} of 30 segments, there is only a slightly higher probability for the macroion to be located in the end. Generally, when a PE_{guest} is added to the system, the binding region becomes broader (except for $N_{seg,guest} = 5$) and the macroion is pushed to one end of the chain. The probable mechanism is that the PE_{guest} complexes to one end of the chain, and when $N_{seg,guest}$ is increased, the PE_{guest} covers more and more segments of the PE_{host} and pushes the macroion to the end of the PE_{host} chain. Finally, when $N_{seg,guest} = N_{seg,host}$, the macroion is totally released.

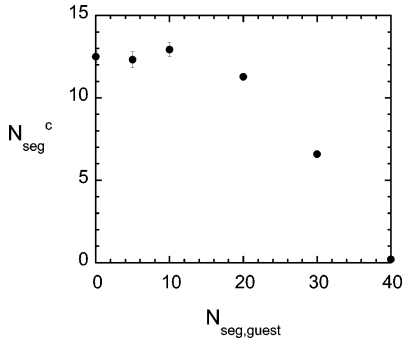

Figure 5. Number of PE_{host} segments within 5 Å from the macroion surface, N_{seg}^c, for the reference system as a function of $N_{seg,guest}$. The estimated uncertainties are smaller than the sizes of the symbols.

The number of PE_{host} segments complexed with a macroion, N_{seg}^c, has also been examined. Figure 5 shows that N_{seg}^c is decreasing when $N_{seg,guest}$ is increasing. In the reference system, approximately 12.5 segments are within 5 Å from the macroion surface. This value is within the statistical uncertainty when $N_{seg,guest} = 0-10$, and then it starts to fall off. When $N_{seg,guest} = 30$, 6.6 segments are within 5 Å, and finally, when $N_{seg,guest} = N_{seg,host}$, the corresponding value is 0.2. Hence, as expected from the results above, the number of PE_{host} segments close to the macroion surface is decreasing when $N_{seg,guest}$ is increasing; that is, the macroion is exchanged by the PE_{guest}.

3.1.3. Polyelectrolyte Conformation. Generally, an undisturbed polyelectrolyte is quite extended, and upon addition of oppositely charged macroion(s), it starts to contract (see ref 29). Figure 6 shows the rms end-to-end separation, $\langle R_{ee}^2 \rangle^{1/2}$, in angstroms, as a function of $N_{seg,guest}$. The first point in the graph ($N_{seg,guest} = 0$, $\langle R_{ee}^2 \rangle^{1/2} = 126$) corresponds to a single undis-

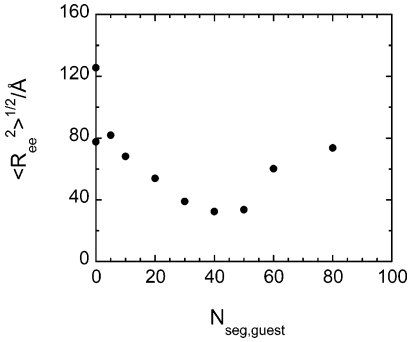

Figure 6. rms end-to-end separation, $\langle R_{ee}^2 \rangle^{1/2}$, of the PE_{host} in angstroms as a function of $N_{seg,guest}$ for the reference system. The estimated uncertainties are smaller than the sizes of the symbols.

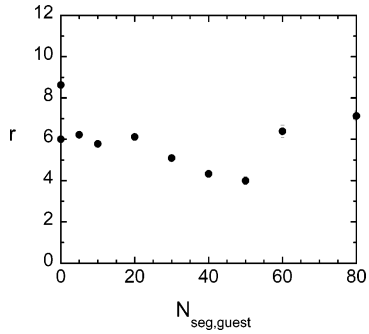

Figure 7. Shape of the PE_{host}, r, as a function of $N_{seg,guest}$ for the reference system. The estimated uncertainties are smaller than the sizes of the symbols.

turbed polyelectrolyte with its counterions, and the second point ($N_{seg,guest} = 0$, $\langle R_{ee}^2 \rangle^{1/2} = 78$) corresponds to the reference system. Complexation of a macroion reduces $\langle R_{ee}^2 \rangle^{1/2}$ from 126 to 78 Å, a decrease by ~40%. The main reason for this contraction is that the polyelectrolyte wraps around the macroion, with several segments in contact with the macroion surface. The PE_{host} is most contracted when $N_{seg,guest} = 40$, and when $N_{seg,guest} > N_{seg,host}$, the PE_{host} starts to extend again. Here the $PE_{host}-PE_{guest}$ complex has become oppositely charged ($\beta > 1$). Similar behavior has been shown for a polyelectrolyte complexed with several macroions.[29] The polyelectrolyte attained its maximum contraction when the polyelectrolyte−macroion complex was charge neutral, and when the polyelectrolyte became overcharged by macroions, the polyelectrolyte extended again, probably due to the repulsion between the complexed macroions.

The ratio of the mean square end-to-end distance to the mean square radius of gyration ($r \equiv \langle R_{ee}^2 \rangle / \langle R_G^2 \rangle$) is a quantity that characterizes the average shape of the polyelectrolyte chain. In the rodlike limit, $r = 12$, whereas, for flexible chains in good solvent, $r \approx 6.3$, and for ideal chains, $r = 6$. The corresponding r for the undisturbed PE_{host} was 8.6; thus, it was more rigid than an ideal chain. Figure 7 shows the shape ratio for the PE_{host} as a function of $N_{seg,guest}$. For $N_{seg,guest} = 0$, the PE_{host} behaves as an ideal chain, and this behavior is attained for shorter PE_{guest}'s. For a neutral $PE_{host}-PE_{guest}$ complex, $r \approx 4$, and for an overcharged $PE_{host}-PE_{guest}$ complex, $r \approx 6.5$; thus, in the absence of an oppositely charged macroion or polyelectrolyte, the PE_{host} is extended, although it is far from being a rigid rod. At $N_{seg,guest} = 40$ ($\beta = 1$), it is collapsed, and when $N_{seg,guest} > 40$ ($\beta > 1$), it becomes more elongated again. Thus, upon complexation, the PE_{host} not only changes its size, that is, contracts, but also changes its shape, that is, becomes less elongated.

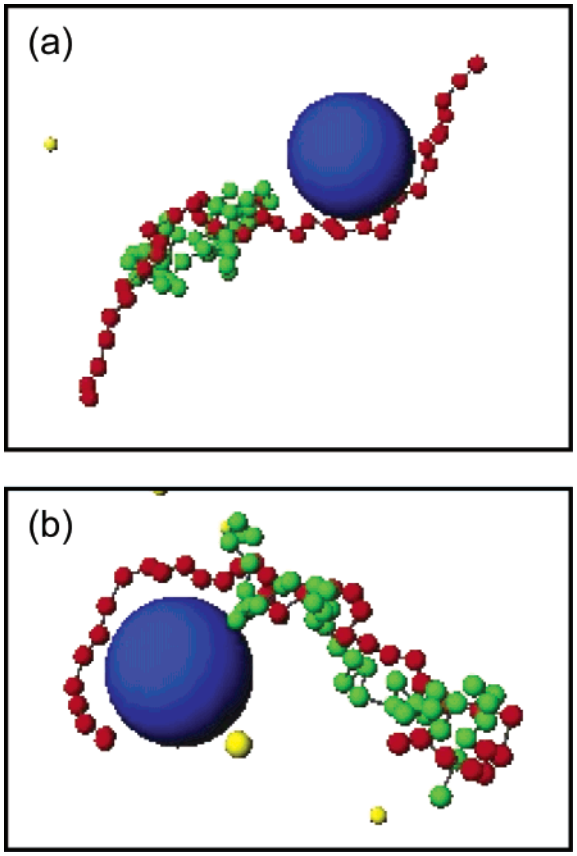

Figure 8. Typical configurations of the complexation between the PE_{host} (connected red dots) with $N_{seg,host} = 40$ and $\tau_{host} = 0.2$ e/Å, the PE_{guest} (connected green dots) with $N_{seg,guest} = 40$, and the macroion (larger blue sphere) with the charge $Z_M = -10$ for the linear charge densities (a) $\tau_{guest} = -0.05$ e/Å and (b) $\tau_{guest} = -0.1$ e/Å of the PE_{guest}. Only a few of the small ions are presented (yellow dots). Note: the parts of the figure are justified for best visibility. The particle sizes in parts a and b are identical.

3.2. Macroion Release. The results given for the reference system above have shown that the macroion will be released when $N_{seg,guest} = N_{seg,host}$. Originating from the reference system and the condition $N_{seg,guest} = N_{seg,host}$, the structures of the systems with different PE_{guest} (i) linear charge densities and (ii) flexibilities have been examined.

3.2.1. Effect of the Linear Charge Density. Figure 8 shows some illustrative snapshots where τ_{guest} is varied but $N_{seg,guest} = N_{seg,host} = 40$. In Figure 8a, $Z_{guest} = -0.25$ when $\tau_{guest} = -0.05$ e/Å, and in Figure 8b, $Z_{guest} = -0.5$ when $\tau_{guest} = -0.1$ e/Å (compare to $Z_{host} = 1.0$ when $\tau_{host} = 0.2$ e/Å). Here it seems that the PE_{host} is able to accommodate both the macroion and the PE_{guest} when τ_{guest} is decreased, which was not the case for $\tau_{guest} = -0.2$ e/Å (see Figure 1c). As was suggested above, a probable mechanism is that when the PE_{guest} is added, it complexes with one end of the PE_{host} and pushes the macroion to the other end of the chain. When τ_{guest} of the PE_{guest} is increased, the PE_{guest} will cover more and more segments of the PE_{host}. When there are charge-matching conditions, one PE_{guest} segment will complex with one PE_{host} segment and the macroion will be released. The complexation probability, $P_j^c(i_{seg})$, between the PE_{host} and the macroion as a function of τ_{guest} is displayed in Figure 9. For $\tau_{guest} = -0.05$ e/Å, the macroion is preferentially located in the central binding region with a slight displacement to the end of the PE_{host}, while, for $\tau_{guest} = -0.1$ e/Å, the macroion is located in the end of the PE_{host}. For the reference system, the complexation function was

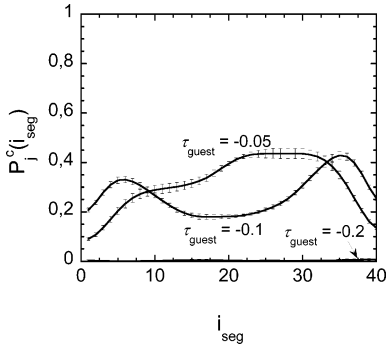

Figure 9. Complexation probability, $P_j^c(i_{seg})$, vs segment rank, i_{seg}, of the PE_{host} for $\tau_{guest} = -0.05$, -0.1, and -0.2 e/Å (see the inset in Figure4f) and $N_{seg,guest} = 40$.

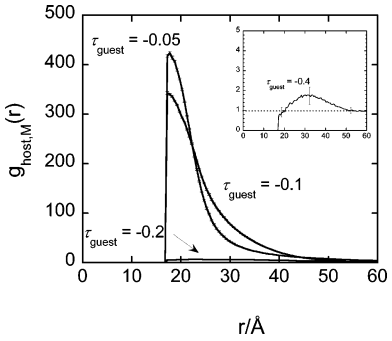

Figure 10. $PE_{host}-M$ rdf, $g_{host,M}(r)$, for $\tau_{guest} = -0.05$, -0.1, and -0.2 e/Å and $N_{seg,guest} = 40$. The inset shows the corresponding rdf for $\tau_{guest} = -0.4$ e/Å, where the horizontal dashed line at $g(r) = 1$ corresponds to uncorrelated distributions.

close to zero; see the inset in Figure 4f. The integral of the complexation probability function provides the average number of PE_{host} segments complexed with the macroion and becomes 12.7, 10.5, and 0.2 for $\tau_{guest} = -0.05$, -0.1, and -0.2 e/Å, respectively.

Figure 10 shows the $g_{host,M}$ for all studied τ_{guest}'s. At $\tau_{guest} = -0.05$ and -0.1 e/Å, a pronounced maximum appears at the contact separation. The magnitude of the maxima decreases as τ_{guest} increases, due to the release of the macroion (less segments in contact with the macroion). The widths of the peaks in Figure 10 support that the firmest complex is created for $\tau_{guest} = -0.05$ e/Å, while the complex becomes looser when τ_{guest} is increased. When $\tau_{guest} = -\tau_{host}$, the macroion is released, although simulations with a PE_{guest} of 20 segments and $\tau_{guest} = -0.4$ e/Å show that the chain length is of minor importance (see the inset in Figure 10). Hence, it is the total charge of the PE_{host} that determines if the macroion shall be released or not, and it is reasonable to assume that the electrostatic interaction is the primary factor controlling the macroion release and the complex composition.

3.2.2. Effect of Chain Flexibility. The influence of the flexibility of the PE_{guest} on the macroion release has been investigated by comparing systems with different flexibilities of the PE_{guest}. Three different bare chain stiffnesses achieved by using the angular force constants $k_{ang} = 0$, 36, and 132.9×10^{-24} J/deg^2 have been applied. The stiffness of a single neutral chain was determined by calculating the average angles between three consecutive segments. The angular force constants used gave $\langle\alpha\rangle = 104$, 167, and 173°, respectively, and the bare persistence lengths $l_p = 7$, 158, and 598, respectively. Hence, the range from flexible to stiff polyelectrolytes is covered (see, e.g., $l_p \approx 400$ Å for DNA). The different systems will be denoted flex, semi, and stiff for the different PE_{guest}'s.

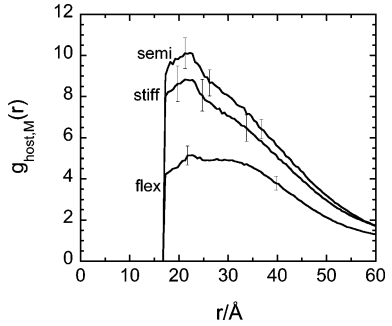

Figure 11. (a) $PE_{host}-M$ rdf, $g_{host,M}(r)$, and (b) $PE_{host}-PE_{guest}$ rdf, $g_{guest,M}(r)$, for different flexibilities of PE_{guest}'s and $N_{seg,guest} = 40$. The denotations on the curves correspond to the bare persistence lengths of flex = 7 Å, semi = 158 Å, and stiff = 598 Å.

Figure 11 shows $g_{host,M}$ for the three systems. Notice that the rdf's for the semiflexible and the stiff chains are, within statistical uncertainty, identical. The rdf's show that the PE_{host} will release its macroion to a larger extent if the PE_{guest} is flexible, while semiflexible and stiff PE_{guest}'s have a similar effect on the macroion release. This result indicates that, after imposing a certain degree of stiffness, nothing is changing. Figure 12 shows an illustrative snapshot for the semi system, while a snapshot for the flex system is given in Figure 1c. Comparison between the snapshots indicates that the polyelectrolyte complexes can be divided into two groups: (i) two oppositely charged flexible chains, which create a compact complex, or (ii) two oppositely charged stiffer chains, which create an elongated complex. This group behavior is further quantified in Table 2, where $\langle R_{ee}^2\rangle^{1/2}$, $\langle R_G^2\rangle^{1/2}$, and the average angle between three consecutive segments, $\langle\alpha\rangle$, are given. The values for the three properties coincide very well for the stiffer chains (compare bold numbers).

Possible explanations to the deviant behavior between groups i and ii upon the macroion release are that the elongated complex will act as a stronger dipole and attract the macroion to a larger extent than the compact complex and, secondly, the PE_{host} in the elongated complex has a larger ability to create tails in the complex and, hence, a higher probability to complex with the macroion.

The tendency of the oppositely charged polyelectrolytes in group ii is to form a more elongated complex, which is a balance between making the opposite charges between the PE_{host} and the PE_{guest} as close to matching as possible, without a high cost in bending energy penalty. When imposing some stiffness onto the PE_{guest}, the compact complex behavior is prevented and the contribution to the free energy from the chain entropy is much less than the contribution from attractive electrostatic interaction between the polyelectrolyte segments. The small deviations between the chain conformational properties are given in Table 2.

Finally, the complexation probability, $P_j^c(i_{seg})$, between the PE_{host} and the macroion as a function of the PE_{guest} flexibility did not provide any extra information. On average, 0.3 PE_{guest} segments were complexed with the macroion surface, and the functions had the same appearance for all analyzed flexibilities (see Figure 4f).

4. Conclusions

Monte Carlo simulations have been performed for model systems representing an aqueous solution containing a $PE_{host}-M$ complex and a varied length of PE_{guest}'s. The macroion and PE_{guest} were oppositely charged compared to the case of the PE_{host}. All the small ions have been treated explicitly.

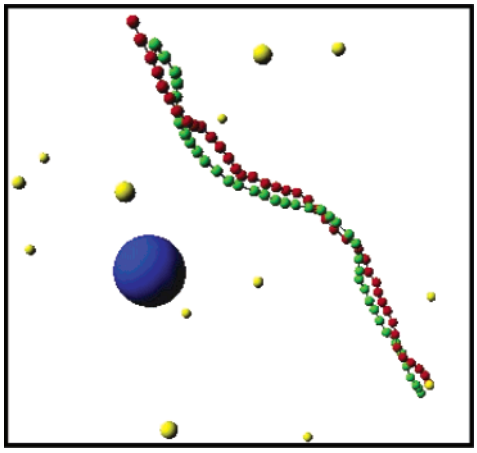

Figure 12. Typical configuration of a system consisting of one flexible PE_{host} (connected red dots) with $N_{seg,host} = 40$ and $\tau_{host} = 0.2$ e/Å, one semiflexible PE_{guest} (connected green dots) with $N_{seg,guest} = 40$ and $\tau_{guest} = -0.2$ e/Å, and one macroion (larger blue sphere) with $Z_M = -10$. Only a few of the small ions are presented (yellow dots).

TABLE 2: Polyelectrolyte Properties of the Simulated Systems Where $\langle R_{ee}^2\rangle^{1/2}$ Is the rms End-to-End Separation (angstroms), $\langle R_G^2\rangle^{1/2}$ is the rms Radius of Gyration (angstroms), and $\langle\alpha\rangle$ is the Average Angle between Three Consecutive Segments (deg)[a]

	PE_{host}/PE_{guest} (flex)	PE_{host}/PE_{guest} (semi)	PE_{host}/PE_{guest} (stiff)
$\langle R_{ee}^2\rangle^{1/2}$	33.0/33.2	35.7/**34.1**	36.8/**34.9**
$\langle R_G^2\rangle^{1/2}$	15.8/15.8	17.9/**18.5**	17.7/**18.3**
$\langle\alpha\rangle$	107.6/107.6	110.1/**149.7**	109.7/**149.9**

[a] Largest estimated uncertainties are $\sigma = 0.3$, 0.1, and 0.1 for $\langle R_{ee}^2\rangle^{1/2}$, $\langle R_G^2\rangle^{1/2}$, and $\langle\alpha\rangle$, respectively.

The main questions were: What is the complex composition and structure, and under what circumstances are the macroion released? When the PE_{guest} is added to a solution consisting of a $PE_{host}-M$ complex, there are three options: (i) $PE_{host}-M + PE_{guest} \rightarrow PE_{host}-M + PE_{guest}$ (nothing changes), (ii) $PE_{host}-M + PE_{guest} \rightarrow PE_{host}-PE_{guest} + M$ (the macroion is exchanged by the guest polyelectrolyte), or (iii) $PE_{host}-M + PE_{guest} \rightarrow PE_{host}-PE_{guest}-M$ (one large complex is created). This study has shown that it is the charge of the PE_{guest} that determines if the macroion is released or not. For $\beta < 1$, one large complex is created (iii), and for $\beta \geq 1$, the macroion is released and a $PE_{host}-PE_{guest}$ complex is created (ii). Hence, case i is never favorable, at least not in this study when $Z_M < Z_{host}$.

In the reference system, the PE_{host} complexes the macroion to its central binding region, with two dangling tails. Besides the exception of the really short PE_{guest}, the binding region gets broader and the tails of the PE_{host} get more involved and, thus, the macroion is pushed to one end of the chain. By varying the chain length and charge, it is shown that the macroion release is an electrostatic effect.

The flexibility of the PE_{guest} has shown peculiar results. It seems that the polyelectrolytes can be divided into two groups: (i) two oppositely charged flexible chains, which create a compact complex, or (ii) two oppositely charged stiffer chains, which create an elongated complex. More importantly, if the main purpose is to release the macroion, one should add a flexible PE_{guest} to the system, while if there are only stiffer chains to access, it is irrelevant which one to choose. This group behavior is probably an effect of the competition between a strong Coulombic interaction, in which the two chains are mixed and each bead interacts with several others, and a bending penalty that induces linearity and essentially lateral proximity or wrapping of the more flexible chain around the stiffer one. When a certain degree of stiffness is imposed (semiflexible and stiff chains in this paper), formation of the compact complex is prevented and the conformational behavior of the complex does not change with increased stiffness.

Although the primitive model is a simple model, it is expected that the physicochemical properties of these kinds of systems are dominated by strong electrostatic interaction. Several simulation studies based on this model have shown good agreement with experimental results.

Acknowledgment. Dr. A. Pais and Prof. T. Arnebrant are greatly acknowledged for valuable discussions. The work was supported by grants from the KK knowledge foundation and by computing resources from LUNARC, Lund University.

References and Notes

(1) Sukhorukov, G. B.; Donath, E.; Davis, S.; Lichtenfield, H.; Caruso, F.; Popov, V. I.; Möhwald, H. *Polym. Adv. Technol.* **1998**, *9*, 759.
(2) Kwak, J. C. T., Ed. *Polymer-Surfactant Systems*; Marcel Dekker: New York, 1998; Vol. 77.
(3) Tsuboi, A.; Izumi, T.; Hirata, M.; Xia, J.; Dubin, P. L.; Kokufuta, E. *Langmuir* **1996**, *12*, 6295.
(4) Xia, J.; Dubin, P. L. In *Macromolecular Complexes in Chemistry and Biology*; Dubin, P., Bock, J., Davis, R., Schulz, D. N., Thies, C., Eds.; Springer-Verlag: Berlin, 1994.
(5) Ganachaud, F.; Elaïssari, A.; Pichot, C.; Laayoun, A.; Cros, P. *Langmuir* **1997**, *13*, 701.
(6) Bielinska, A. U.; Chen, C.; Johnson, J.; Baker, J. R. *Bioconjugate Chem.* **1999**, *10*, 843.
(7) Luger, K.; Mader, A. W.; Richmond, R. K.; Sarget, D. F.; Richmond, T. J. *Nature* **1997**, *389*, 251.
(8) Widom, J. *Annu. Rev. Biophys. Biomol. Struct.* **1998**, *27*, 258.
(9) Goddard, E. D. *Collids Surf.* **1986**, *19*, 301.
(10) Lindman, B.; Thalberg, K. In *Interactions of Surfactants with Polymers and Proteins*; Goddard, E. D., Ananthapadmanabhan, K. P., Eds.; CRC Press: Boca Raton, FL, 1993; p 203.
(11) Hansson, P.; Lindman, B. *Curr. Opin. Colloid Interface Sci.* **1996**, *1*, 604.
(12) Wallin, T.; Linse, P. *Langmuir* **1996**, *12*, 305.
(13) Wallin, T.; Linse, P. *J. Phys. Chem.* **1996**, *100*, 17873.
(14) Wallin, T.; Linse, P. *J. Phys. Chem. B* **1997**, *101*, 5506.
(15) Wallin, T.; Linse, P. *J. Chem. Phys.* **1998**, *109*, 5089.
(16) Akinchina, A.; Linse, P. *Macromolecules* **2002**, *35*, 5183.
(17) Akinchina, A.; Linse, P. *J. Phys. Chem. B* **2003**, *107*, 8011.
(18) Chodanowski, P.; Stoll, S. *J. Chem. Phys.* **2001**, *115*, 4951.
(19) Chodanowski, P.; Stoll, S. *Macromolecules* **2001**, *34*, 2320.
(20) Kong, C. Y.; Muthukumar, M. *J. Chem. Phys.* **1998**, *109*, 1522.
(21) Netz, R. R.; Joanny, J.-F. *Macromolecules* **1999**, *32*, 9026.
(22) Kunze, K.-K.; Netz, R. R. *Phys. Rev. E* **2002**, *66*, 011918.
(23) Nguyen, T. T.; Shklovskii, B. I. *Physica A* **2001**, *293*, 324.
(24) Schiessel, H.; Bruinsma, R.; Gelbart, W. M. *J. Chem. Phys.* **2001**, *115*, 7245.
(25) Mateescu, E. M.; Jeppesen, C.; Pincus, P. *Europhys. Lett.* **1999**, *46*, 493.
(26) Gurovitch, E.; Sens, P. *Phys. Rev. Lett.* **1999**, *82*, 339.
(27) von Goeler, F.; Muthukumar, M. *J. Chem. Phys.* **1994**, *100*, 7796.
(28) Park, S. Y.; Bruinsma, R. F.; Gelbart, W. M. *Europhys. Lett.* **1999**, *46*, 454.
(29) Jonsson, M.; Linse, P. *J. Chem. Phys.* **2001**, *115*, 3406.
(30) Jonsson, M.; Linse, P. *J. Chem. Phys.* **2001**, *115*, 10975.
(31) Skepö, M.; Linse, P. *Phys. Rev. E* **2002**, *66*.
(32) Nguyen, T. T.; Shklovskii, B. I. *J. Chem. Phys.* **2001**, *114*, 5905.
(33) Nguyen, T. T.; Shklovskii, B. I. *J. Chem. Phys.* **2001**, *115*, 7298.
(34) Skepö, M.; Linse, P. *Macromolecules* **2003**, *36*, 508.
(35) Hayashi, Y.; Ullner, M.; Linse, P. *J. Phys. Chem. B* **2003**, *107*, 8198.
(36) Allen, M. P.; Tildesley, D. J. *Computer Simulations of Liquids*; Oxford: New York, 1987.
(37) Frenkel, D.; Smit, B. *Understanding Molecular Simulation*; Academic Press: New York, 1996.
(38) Hayashi, Y.; Ullner, M.; Linse, P. *J. Chem. Phys.* **2002**, *116*, 6836.
(39) Linse, P. *MOLSIM*, 3.4 ed.; Lund University: Sweden, 1999.
(40) The bare persistence length was calculated according to $l_p = \langle R_{seg,seg}^2\rangle^{1/2}/(1 + \langle\cos\alpha_i\rangle)$ for the corresponding uncharged, isolated chain, where $\langle R_{seg,seg}^2\rangle^{1/2}$ is the rms segment−segment separation.